INVESTIGATIONS OF THE ELECTRON BEAM ENERGY JITTER GENERATED IN THE PHOTOCATHODE RF GUN AT THE ADVANCED PHOTON SOURCE LINAC*

J. Dooling†, Y. Sun, D. Hui‡, A. Lumpkin, K. P. Wootton, A. Zholents, T. Smith
Argonne National Laboratory, Lemont, IL USA

Abstract

Characterizations continue of the electron beam properties of a recently installed S-band photocathode (PC) rf gun at the Advanced Photon Source Linac facility. In this case, we have utilized a low-energy spectrometer beam line located 1.3 m downstream of the gun cavity to measure the electron beam energy, energy spread, and energy jitter. The nominal energy was 5.4 MeV using a gun gradient of 110 MV/m, and the energy spread was 17 keV when driven by a 2.5-ps rms duration UV laser pulse at the selected rf gun phase. An energy jitter of 25 keV was initially observed in the spectrometer focal plane images. This jitter was partly attributed to the presence of both the 2nd and 3rd harmonics of the 119 MHz synchronization signal provided to the phase locked loop of the drive laser oscillator. (The nominal rms jitter from the timing stabilizer is 1.6 ps.) The addition of a 150-MHz low-pass filter in the 119-MHz line strongly attenuated the two harmonics and resulted in a reduced energy jitter of 15 keV. Comparisons of the gun performance to ASTRA simulations will also be presented.

INTRODUCTION

Installation of an LCLS-I-style, dual-waveguide-feed photocathode (PC) gun at the upstream end of the Advanced Photon Source (APS) linac was completed in 2015. A spectrometer line is included with the PC Gun to allow measurement of gun energy and energy spread. A YAG screen and current monitor upstream of the spectrometer dipole magnet enables solenoid-scan emittance and quantum efficiency measurements as well. The spectrometer dipole magnet current is interlocked to permit parallel operation of the PC Gun with user beam. A schematic of the PC Gun beam line is presented in Figure 1. For upcoming experiments overlapping photon and electron beams, e.g. tapering enhanced stimulated superradiant amplification (TESSA) [1,2], requirements are rms jitter <300 fs and peak current >1 kA.

ANALYSIS

While measuring beam energy using the YAG screen at the end of the spectrometer line (YAGBend), fluctuations in horizontal position were observed. Motion of the laser spot on the cathode, as measured on the virtual cathode (VC),
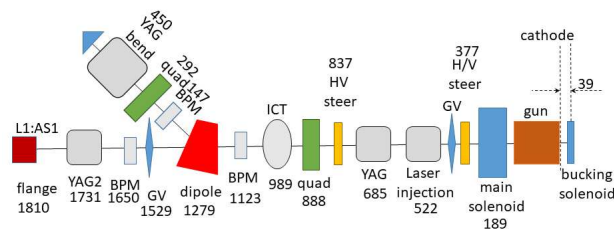
Figure 1: APS PC Gun beam line schematic.

is small. An image from the VC covering 2 mm x 2 mm is shown in Figure 2. Over a 5-minute interval, the spot
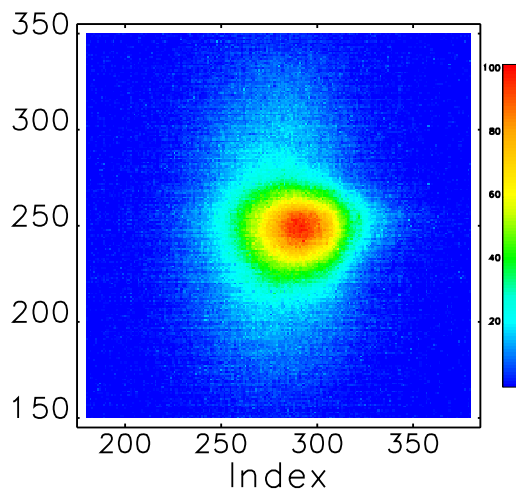

Figure 2: Laser spot on the VC camera; rms x- and y-spot sizes are 0.24 mm and 0.22 mm. FOV: 2 mm x 2 mm.

centroid was observed to vary by 8 μm. Dispersion in the spectrometer line suggests the fluctuations are due to energy variations which are in turn caused by differences between the arrival time of the laser pulse and phase of the rf on the gun photocathode surface. The energy fluctuations or jitter can be determined once the dispersion at the YAGBend screen is known; the dispersion will be modified by the quadrupole magnet just upstream of the screen.

Dispersion

Examining the x-z components of the transfer matrix from the entrance of the dipole to YAGBend,

$$\vec{x}_1 = \boldsymbol{R}_s \vec{x}_0, \tag{1}$$

where R_s includes the effects of the drift, quadrupole (thin lens), and sector bend elements [3],

$$R_s = R_{l2}R_qR_{l1}R_{bm} \qquad (2)$$

Writing the elements for R_s generally as,

$$\begin{vmatrix} x_1 \\ x_1' \\ z_1 \\ \delta_1 \end{vmatrix} = \begin{vmatrix} A & B & C & D \\ E & F & G & H \\ I & J & K & L \\ M & N & O & P \end{vmatrix} \begin{vmatrix} x_0 \\ x_0' \\ z_0 \\ \delta_0 \end{vmatrix} \qquad (3)$$

find,

$$x_1 = Ax_0 + Bx_0' + Cz_0 + D\delta_0. \qquad (4)$$

From inspection, we see that D is equivalent to the horizontal dispersion, D_x. The dispersion may be expressed as,

$$D_x = 2\rho \sin^2\left(\frac{\theta}{2}\right) + (l_1 + l_2)\sin(\theta) \\ + kl_2 \sin(kl_e)\left[2\rho \sin^2\left(\frac{\theta}{2}\right) + l_1 \sin(\theta)\right], \quad (5)$$

where, $k^2 = (B_o/a)/(\rho B)$ and l_e is the effective length of the quadrupole; in addition, a is the pole-tip radius, ρB is the magnetic rigidity, and $B_o/a = dB/dx$ is the field gradient [4]. The distance from the vertex of the dipole magnet to the exit is 60 mm; subtracting this length from the drift distance to the quadrupole shown in Fig. 1, we find $l_1 = 232$ mm. Also, $l_2 = 158$ mm, $\theta = \pi/4$, and $\rho = 150$ mm. For the quadrupole magnet with current, $I_q = 3.4$ A, $k = 10.74$ m^{-1} and $l_e = 0.0773$ m. Inserting these values into Eq. 5, find $D_x = 0.059$ m; in the limit where $k \to 0$, $D_x = 0.32$ m. (Note: because $kl_e \sim 1$, a thick lens model is more appropriate; the thin-lens model provides a initial estimate of D_x.)

Measurements of $D_x \approx p/(\Delta p/\Delta x)$ indicate the dispersion to be approximately 135 mm near the center of the YAGBend screen as shown in Figure 3.
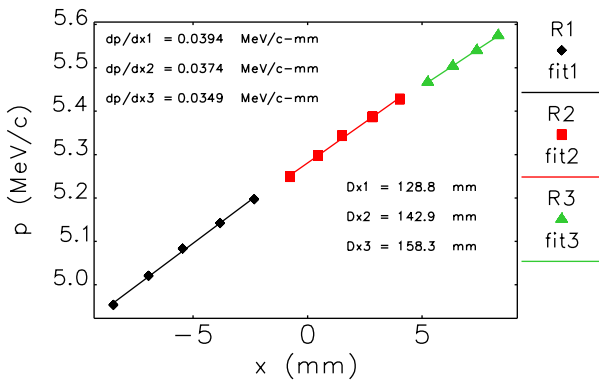

Figure 3: Dispersion measurements at YAGBend.

ASTRA Simulation

ASTRA [5] simulations have been run to model beam energy versus phase. A simulated phase scan for an rf power level at the gun of 10 MW (peak gradient $E = 116$ MV/m) is presented in Figure 4. The coefficients for the fit are given in the figure. A fourth-order polynomial is used to fit [6] the
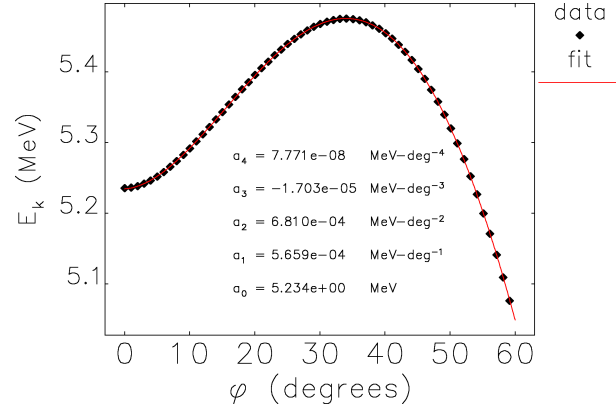

Figure 4: Beam energy versus phase from an ASTRA phase scan for $E = 116$ MV/m. A polynomial fit and fit coefficients are also shown.

simulation results,

$$E_k(\phi) = a_4\phi^4 + a_3\phi^3 + a_2\phi^2 + a_1\phi + a_0 \qquad (6)$$

The gun is typically operated between 30° and 45°; in this case, we set $\phi = 43°$. From Eq. 6, we find $E_k(\phi = 43°) = 5.43$ MeV and $dE_k(\phi)/d\phi = 0$ at $\phi = 34.03°$. Differentiating Eq. 6, $dE_k/d\phi|_{\phi=43°} = 10.4$ keV/°. Converting to a variation with phase,

$$\frac{dE_k(\phi)}{dt} = \left(\frac{d\phi}{dt}\right)\left(\frac{dE_k(\phi)}{d\phi}\right) = \omega\frac{dE_k(\phi)}{d\phi}, \qquad (7)$$

where $\omega = 2\pi(2856$ MHz$)$, $dE_k/dt|_{\phi=43°} = 10.1$ keV/ps.

MEASUREMENTS

The APS PC Gun drive laser is an Nd:Glass-based, chirped pulse amplifier (CPA) system [7] utilizing a Lumentum (formerly Time Bandwidth) GLX-200 mode-locked oscillator [8, 9]. The oscillator in turn uses a CLX-1000 timing stabilizer locked to 119 MHz, the 24th subharmonic of the linac 2856 MHz s-band frequency. Recent solenoid-scan and three-screen emittance measurements in the linac chicane section have shown an increase in fluctuations of the electron beam size especially near the minimum. A schematic of the timing stabilizer and oscillator and locations where measurements were made around these components is presented in Figure 5.

The rf input to the timing stabilizer was recorded on an oscilloscope; an FFT analysis was applied to the time data to examine the spectral content. The FFT revealed significant noise at the 2nd and 3rd harmonics of 119 MHz. Adding a low-pass filter (LPF, MiniCircuits SLP-150) reduced these
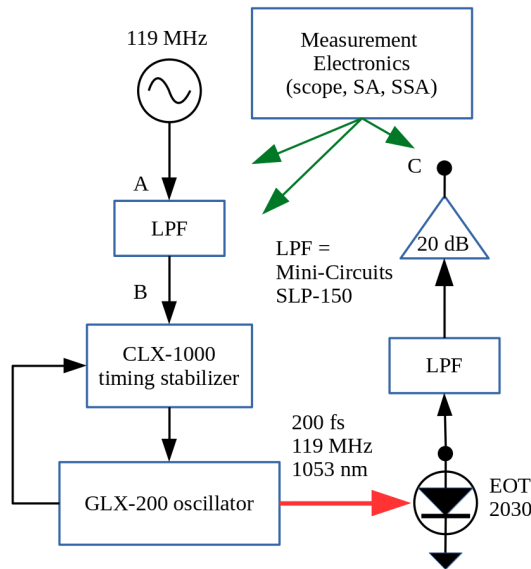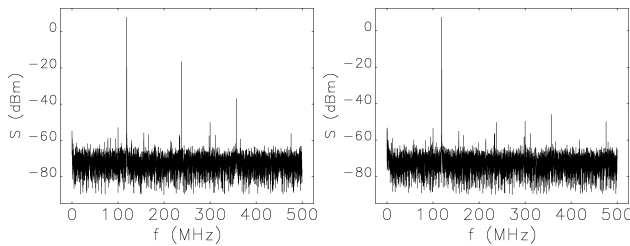
Figure 5: Timing stabilizer and oscillator schematic.

(a) Without low-pass filtering.   (b) With a 150 MHz LPF.

Figure 6: Spectra of the 119 MHz reference rf signal used to phase-lock the oscillator timing stabilizer a) without and b) with a LPF upstream of the stabilizer.

harmonic components as shown in Figure 6. Measurements of centroid position at the YAGBend screen showed a reduction in jitter after the LPF was installed. Prior to installation of the LPF, the centroid standard deviation was found to be 24.4 pixels (1.63 mm); after installation the standard deviation fell to 14.1 pixels (0.94 mm). Converting position fluctuations on the YAGBend screen to energy variations and then to timing jitter, centroid versus time is plotted in Figure 7. A histogram of the occurrence frequency shows two distinct peaks in Δt. The histogram was generated with a bin width of 0.15 ps and indicates a jitter of 0.99 ps, rms. The data in Fig. 7 was collected with the LPF in place. Jitter observed on the spectrometer screen can come from other sources in addition to that from the laser including phase and amplitude fluctuations on the rf drive signal, field variations in the magnets, and bunch profile modifications. We assume magnetic field and bucnch profile fluctuations to be small. Phase noise on the rf drive signal was measured to be 0.143°, rms; this leads to an error of approximately 14% on the jitter number given above.

An Agilent E5052B Signal Source Analyzer (SSA) was used to assess the rms jitter in both the 119-MHz rf reference
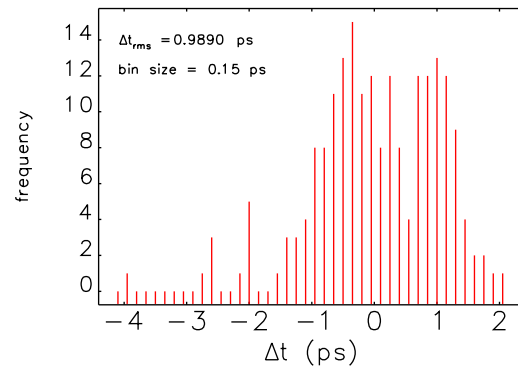

Figure 7: Jitter measurement at YAGBend.

timing stabilizer input signal and the detected output of the mode-locked cw oscillator, see Fig. 5. Power spectral density waveforms for both signals are shown in Figure 8; in both cases the LPF is inserted at the reference input to the CLX-1000 timing stabilizer.
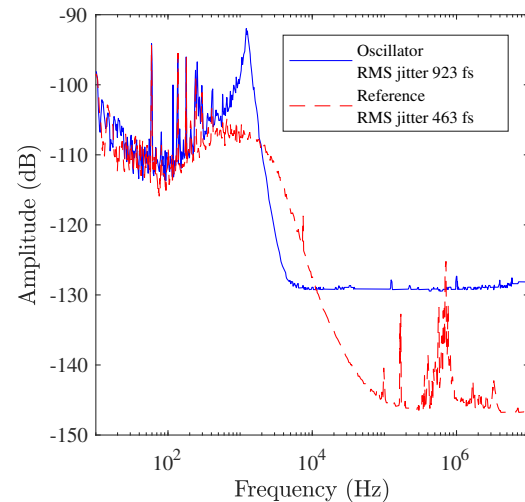

Figure 8: Power spectral density waveforms of the 119-MHz reference rf and detected mode-locked oscillator output. In both cases, a 150-MHz LPF is inserted ahead of the timing stabilizer rf input. Carrier power is 7.56 dBm at the input to the stablilzer and -9.94 dBm at the output of the diode (points B and C in Fig. 5).

SUMMARY

Rms jitter measurements made with the E5052B SSA are consistent with the jitter result obtained from the spectrometer bend line. Effort will be required to reduce the rms jitter of the drive laser oscillator to the 300 fs level.

ACKNOWLEDGMENTS

REFERENCES

[1] J. P. Duris *et al.*, "Tapering enhanced stimulated superradiant amplification," *New J Phys*, vol. 17, p. 063036, June 2015.

[2] N. Sudar *et al.*, "High Efficiency Energy Extraction from a Relativistic Electron Beam in a Strongly Tapered Undulator," *Phys Rev Lett*, vol. 117, p. 174801, October 2016.

[3] H. Wiedemann, *Particle Accelerator Physics*. Springer, 3rd ed., 2007.

[4] K. Brown. A. Chao *et al.*, eds., *Handbook of Accelerator Physics and Engineering*, 3rd ed., 2006, p. 72, Section 2.2.1.

[5] K. Flöttmann, www.desy.de/~mpyflo

[6] M.Borland, "User's Guide for SDDS Toolkit."

[7] Y. Li. ANL/APS/LS-307, APS, 2008.

[8] https://www.photonicsolutions.co.uk/upfiles/glx-200-web.pdf

[9] N. Stuart *et al.*, "Comparative study on the temporal contrast of femtosecond mode-locked laser oscillators," *Optics Letters*, vol. 41, Issue 14, p. 3221, 2016.